

# Analysis on diurnal global geomagnetic variability under quiet-time conditions

Virginia Klausner<sup>1,\*</sup>

*DGE/CEA/National Institute for Space Research - phone: +55 12 32086819/fax: +55 12 32086810 - INPE 12227-010 São José dos Campos, SP, Brazil.*

Margarete Oliveira Domingues

*LAC/CTE/National Institute for Space Research - phone: +55 12 32086542/fax: +55 12 32086375 - INPE 12227-010 São José dos Campos, SP, Brazil*

Odim Mendes Jr

*DGE/CEA/National Institute for Space Research - phone: +55 12 32087854/fax: +55 12 32086810 - INPE 12227-010 São José dos Campos, SP, Brazil*

Andres Reinaldo Rodriguez Papa<sup>2</sup>

*National Observatory - phone: +55 21 35049142/fax: +55 21 25807081 - ON 20921-400, RJ, Brazil*

Peter Frick

*Laboratory of Physical Hydrodynamics - phone: +7 342 2378322/fax: +7 342 2378487 - Institute of Continuous Media Mechanics, Perm, Russia*

---

## Abstract

This paper describes a methodology (or treatment) to establish a represen-

---

\*Corresponding author

*Email addresses:* [virginia@dge.inpe.br](mailto:virginia@dge.inpe.br) (Virginia Klausner), [mo.domingues@lac.inpe.br](mailto:mo.domingues@lac.inpe.br) (Margarete Oliveira Domingues), [odim@dge.inpe.br](mailto:odim@dge.inpe.br) (Odim Mendes Jr), [papa@on.br](mailto:papa@on.br) (Andres Reinaldo Rodriguez Papa), [frick@icmm.ru](mailto:frick@icmm.ru) (Peter Frick)

<sup>1</sup>National Observatory - ON 20921-400, RJ, Brazil.

<sup>2</sup>State University of Rio de Janeiro - UERJ 20550-900, RJ, Brazil

tative signal of the global magnetic diurnal variation based on a spatial distribution in both longitude and latitude of a set of magnetic stations as well as their magnetic behavior on a time basis. For that, we apply the Principal Component Analysis (PCA) technique implemented using gapped wavelet transform and wavelet correlation. The continuous gapped wavelet and the wavelet correlation techniques were used to describe the features of the magnetic variations at Vassouras (Brazil) and other 12 magnetic stations spread around the terrestrial globe. The aim of this paper is to reconstruct the original geomagnetic data series of the H-component taking into account only the diurnal variations with periods of 24 hours on geomagnetically quiet days. With the developed work, we advance a proposal to reconstruct the baseline for the quiet day variations (Sq) from the PCA using the correlation wavelet method to determine the global variation of PCA first mode. The results showed that this goal was reached and encourage other uses of this approach to different kinds of analysis.

*Keywords:* Magnetogram data, H-component, Quiet days, Principal Component Wavelet analysis.

---

## 1. Introduction

2 A substantial part of the energy carried by the solar wind can be trans-  
3 ferred into the terrestrial magnetosphere and it is associated with the passage  
4 of southward directed interplanetary magnetic fields,  $B_s$ , by the Earth for suf-  
5 ficiently long intervals of time. Gonzalez et al. (1994) discussed the energy  
6 transfer process as a conversion of the directed mechanical energy from the  
7 solar wind into magnetic energy stored in the magnetotail of Earth's magne-

8    tosphere and its reconversion into thermal mechanical energy in the plasma  
9    sheet, auroral particles, ring current, and Joule heating of the ionosphere.

10    The increase on the solar wind pressure is responsible for the energy in-  
11    jections and induces global effects in the magnetosphere called geomagnetic  
12    storms. The characteristic signature of geomagnetic storms can be described  
13    as a depression on the horizontal component of the Earth's magnetic field  
14    measured at low and middle latitude ground stations. The decrease in the  
15    magnetic horizontal field component is due to an enhancement of the trapped  
16    magnetospheric particle population, consequently an enhanced ring of cur-  
17    rent. This perturbation of the H-component could last from several hours to  
18    several days (as described by Kamide et al., 1998).

19    The geomagnetic storms can consist of four phases: sudden commence-  
20    ment, initial phase, main phase and recovery phase. The sudden commence-  
21    ment when it exists, corresponds to the moment when the initial impact of  
22    the increased solar wind pressure over the magnetopause occurs. The ini-  
23    tial phase at ground appears as a rapid increase on the H-component over  
24    less than 1 h almost simultaneously worldwide. The main phase of the ge-  
25    omagnetic storm lasts a few hours and is characterized by a decrease in the  
26    H-component. The recovery time corresponds to the gradual increase of the  
27    H-component value to its average level. A detailed description of the mor-  
28    phology of magnetic storms is, for instance, in Gonzalez et al. (1994).

29    The intensity of the geomagnetic disturbance in each day is described  
30    by indices. The indices are very useful to provide the global diagnostic of  
31    the degree of disturbance level. There are different indices that can be used  
32    depending on the character and the latitude influences in focus. Considering

33 only the main latitudinal contributions, the ring current dominates at low  
 34 and middle latitudes and an auroral ionospheric current systems dominates  
 35 at higher latitudes (Mendes et al., 2005a). Kp, AE and Dst and their deriva-  
 36 tions are the most used geomagnetic indices. The Kp index is obtained from  
 37 the H-component and it is divided in ten levels from 0 to 9 corresponding to  
 38 the mean value of the disturbance levels within 3-h intervals observed at 13  
 39 subauroral magnetic stations (see Bartels, 1957). However, the K index is  
 40 the most difficult to be physically interpreted due to its variations be caused  
 41 by any geophysical current system including magnetopause currents, field-  
 42 aligned currents, and the auroral electrojets (Gonzalez et al., 1994). The  
 43 minutely AE index (sometimes 2.5 minute interval) is also obtained by the  
 44 H-component measured from magnetic stations (5 to 11 in number) located  
 45 at auroral zones and widely distributed in longitude. The AE index provides  
 46 a measure of the overall horizontal auroral oval current strength. The index  
 47 most used in low and mid-latitudes is the Dst index. It represents the varia-  
 48 tions of the H-component due to changes of the ring current and is calculated  
 49 every hour.

50 The Dst index is described as a measure of the worldwide derivation  
 51 of the H-component at mid-latitude ground stations from their quiet days  
 52 values. At mid-latitude, the H-component is a function of the magnetopause  
 53 currents, the ring current and tail currents. Burton et al. (1975) calculated  
 54 the Dst index as a average of the records from  $N$  mid-latitude magnetic  
 55 stations following,

$$Dst = \frac{1}{N} \sum_{i=1}^N H_{disturbed} - H_{quiet} = \overline{\Delta H} \quad (1)$$

56 where  $\overline{\Delta H}$  is a local time H average,  $H_{disturbed}$  is the H-component mea-  
 57 sured at disturbed days and  $H_{quiet}$ , on quiet days.

58 Other contributions beyond the ring current could be extracted or elim-  
 59 inated with the idea presented by Burton et al. (1975). Those authors de-  
 60 scribed the evolution of the ring current by a simple first order differential  
 61 equation,

$$\frac{d Dst^*}{dt} = Q(t) - a Dst^*, \quad (2)$$

62 where  $Dst^* = Dst - b Pdyn^{\frac{1}{2}} + c$ . The contribution of the magnetopause  
 63 currents to  $H$  is proportional to the square root of the solar wind dynamic  
 64 pressure ( $Pdyn$ ),  $Q$  represents the injection of particles to the ring current,  
 65  $a Dst^*$  represents the loss of particles with an e-folding time  $\frac{1}{a}$  and the con-  
 66 stant terms  $a$ ,  $b$  and  $c$  are determine by the quiet days values of the magne-  
 67 topause and ring currents.

68 The Dst index is available on the Kyoto World Data Center at [http://](http://wdc.kugi.kyoto-u.ac.jp/dstdir/index.html)  
 69 [wdc.kugi.kyoto-u.ac.jp/dstdir/index.html](http://wdc.kugi.kyoto-u.ac.jp/dstdir/index.html). It is traditionally calculated from  
 70 four magnetic observatories: Hermanus, Kakioka, Honolulu, and San Juan.  
 71 These observatories are located at latitudes below  $40^\circ$  which are sufficiently  
 72 distant from the auroral electrojets. The derivation of the Dst index corre-  
 73 sponds to three main steps: the removal of the secular variation, the elimi-  
 74 nation of the Sq variation and the calculation of the hourly equatorial Dst  
 75 Index (see <http://wdc.kugi.kyoto-u.ac.jp/dstdir/dst2/onDstindex.html>).

76 The traditional method of calculating the baseline for the quiet day vari-  
 77 ations uses the five quietest day for each month for each magnetic observa-  
 78 tory. In this work, we propose a way to deal with Sq variations by suggesting

79 a method using Principal Component with the wavelet correlation matrix.  
80 This method eliminates the disturbed days using a multiscale process. Also,  
81 we developed an algorithm for extracting the solar quiet variations recorded  
82 in the magnetic stations time series, in order words, a way of estimation of  
83 the quiet-time baseline. To accomplish this task, we separate the solar di-  
84 urnal variations using hourly data of the H-component using the technique  
85 (described in Klausner et al., 2011a). Afterward we applied the principal  
86 component wavelet analysis to identify the global patterns in the solar diur-  
87 nal variations.

88 The rest of the paper is organized as follows: Section 2 is devoted to  
89 explain the main issues of the Dst index calculation procedure. In Section 3  
90 the analyzed period and data are presented. Section 4 describes the principal  
91 component analysis and it is devoted to introduce the suggested method of  
92 principal component analysis (PCA) using gapped wavelet transform and  
93 wavelet correlation. It also establishes the identification of the disturbed  
94 days. The results are discussed in Section 5, and finally, Section 6 brings the  
95 conclusions of this work.

## 96 **2. The Dst index calculation procedure**

97 Recently, reconstructing the Dst and removing the quiet-time baseline  
98 have been a motivation of several works (Karinen and Mursula, 2005; Mendes et al.,  
99 2005a; Karinen and Mursula, 2006; Mursula et al., 2008; Love and Gannon,  
100 2009; Klausner et al., 2011a). Despite of these disagreements in the Dst con-  
101 struction, today, the Dst index remains an important tool in the space weather  
102 analysis.

103 Karinen and Mursula (2005) reconstructed the Dst index (Dxt) follow-  
104 ing the original formula presented at [http://wdc.kugi.kyoto-u.ac.jp /dst-](http://wdc.kugi.kyoto-u.ac.jp/dst-dir/dst2/onDstindex.html)  
105 [dir/dst2/onDstindex.html](http://wdc.kugi.kyoto-u.ac.jp/dst-dir/dst2/onDstindex.html). However, they encountered a few issues as: the  
106 availability and the data quality , some shifts in the baseline level of the  
107 H-component, erroneous data points and some data gaps at all/some mag-  
108 netic observatories. The Dst could not be fully reproduced using the original  
109 formula because the inadequate information above effects the treatment of  
110 the related issues and therefore remains partly unscientific as described by  
111 Karinen and Mursula (2005).

112 A new corrected and extended version (Dcx) of the Dxt index was pro-  
113 posed by Karinen and Mursula (2006). They corrected the Dst index for the  
114 excessive seasonal varying quiet-time level which was unrelated to magnetic  
115 storms as previously discussed in Karinen and Mursula (2005). They also  
116 showed that the considerable amount of quiet-time variation is included in  
117 the Dxt index but none in the Dcx index.

118 Another issue related to the derivation of the Dst index is that no treat-  
119 ment is made to normalize the different latitudinal location of the magnetic  
120 observatories. Mursula et al. (2008) suggested the normalization of the mag-  
121 netic disturbances at the four Dst stations with different latitudes by the co-  
122 sine of the geomagnetic latitude of the respective station. If no correction is  
123 made, they showed for the lowest geomagnetic station, Honolulu, the largest  
124 deviations and for the highest station, Hermanus, the lowest deviations of  
125 the four station. The standard deviations reflect the annually averaged ef-  
126 fect of the (mainly ring current related) disturbances at each station, (see  
127 Mursula et al., 2008, for more details).

128       Mendes et al. (2005a) evaluated the effect of using more than four mag-  
129 netic stations and shorter time intervals to calculate the Dst index. The  
130 obtained Dst index profiles using 12, 6 or 4 magnetic station did not show  
131 significant discrepancies and the best agreement with the standart Dst was  
132 obtained using magnetic stations located at latitudes lower than  $35^\circ$  in both  
133 hemispheres.

134       Although, the increase of symmetrically world-wide distributed magnetic  
135 stations did not effect significantly the Dst index, the longitudinal asymme-  
136 tries of the ring current contributes for the average disturbances of the Four  
137 Dst stations be systematically different. Mursula et al. (2010) using an ex-  
138 tended network of 17 stations, demonstrated that the local disturbances are  
139 ordered according to the station's geographic longitude, where the western-  
140 most station (Honolulu) presented the largest disturbances and contributions  
141 to Dst index and the easternmost (Kakioka) the smallest.

142       Klausner et al. (2011a) studied the characteristics of the Sq variations at  
143 a Brazilian station and compared to the features from other magnetic sta-  
144 tions to better understand the dynamics of the diurnal variations involved in  
145 the monitoring of the Earth's magnetic field. They used gapped wavelet anal-  
146 ysis and the wavelet cross-correlation technique to verify the latitudinal and  
147 longitudinal dependence of the diurnal variations. As previously mentioned  
148 by Mursula et al. (2010), Klausner et al. (2011a) also verified that magnetic  
149 stations located at lower latitudes and westernmost (Honolulu and San Juan)  
150 presented larger correlation to Vassouras than the easternmost stations (as  
151 Kakioka).

152       Some important aspects for the construction of the Dst index as described



153 by Love and Gannon (2009) are: the utilization of the original data, the in-  
154 spection in time and frequency domains (removal of diurnal variation) and  
155 the consideration of the distinction between stationary and non-stationary  
156 time series ingredients which applies to the secular variation. Also as men-  
157 tioned by Love and Gannon (2009), some patterns of the global magnetic  
158 disturbance field are well understood and some are not which means that  
159 there is still a lot to learn about the magnetosphere, magnetic storm and  
160 Earth-Sun relationship.

### 161 **3. Magnetic Data**

162 In this paper, we use ground magnetic measurements to estimate the  
163 quiet-time baseline. We select the four magnetic observatories used to cal-  
164 culate the Dst index: Hermanus (HER), Kakioka (KAK), Honolulu (HON),  
165 and San Juan (SJG), plus other 9 different magnetic observatories reasonably  
166 homogeneously distributed world wide. One of these nine chosen stations is  
167 Vassouras (VSS) located under the South Atlantic Magnetic Anomaly (min-  
168 imum of the geomagnetic field intensity). The geomagnetic data use in this  
169 work relied on data collections provided by the INTERMAGNET programme  
170 (<http://www.intermagnet.org>).

171 The distribution of the magnetic stations, with their IAGA codes, is given  
172 in Fig. 1. The corresponding codes and locations are given in Table 1. These  
173 selection of magnetic stations correspond to the same selection used in a  
174 previous work o(Klausner et al., 2011a) for the same reasons (exclusion of  
175 the major influence of the auroral and equatorial electrojets). In this work,  
176 we only use the data interval corresponding to the year 2007. We also ap-

177 ply the same methodology to identify geomagnetically quiet days used by  
178 Klausner et al. (2011a). We consider quiet days, only those days in which  
179 the Kp index is not higher than 3+.

180 As at low latitudes the horizontal component (H) is mostly affected by  
181 the intensity of the ring current, we decided to use only the hourly mean  
182 value series of this component. The magnetic stations present available data  
183 in Cartesian components (XYZ system). The Conversion to horizontal-polar  
184 components (HDZ system) is very simple (see Campbell, 1997, for more  
185 details). The system's conversion was performed in all the chosen magnetic  
186 stations.

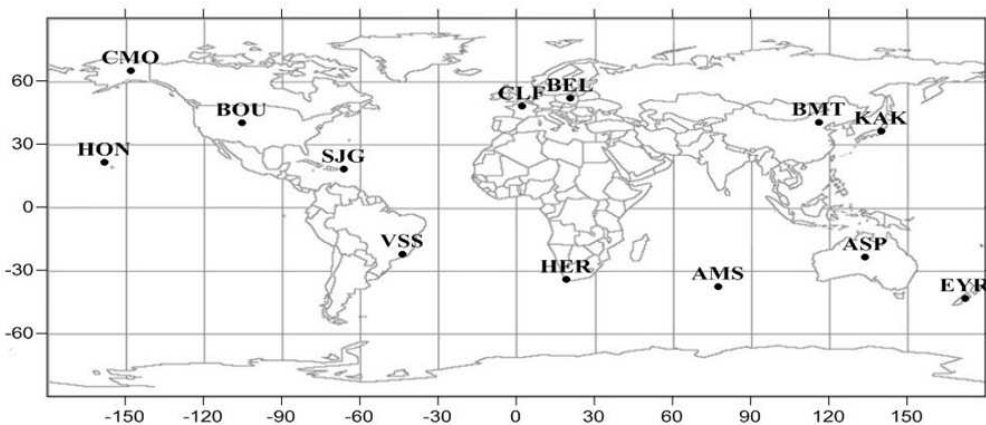


Figure 1: Geographical localization of the stations used in this work and their respective IAGA code.

#### 187 4. Methodology

188 The method used in this study is based on the principal component analy-  
189 sis (PCA) using gapped wavelet transform and wavelet correlation to charac-

Table 1: INTERMAGNET network of geomagnetic stations used in this study.

Station	Geographic coord.		Geomagnetic coord.	
	Lat.( $^{\circ}$ )	Long.( $^{\circ}$ )	Lat.( $^{\circ}$ )	Long.( $^{\circ}$ )
AMS	-37.83	77.56	-46.07	144.94
ASP	-23.76	133.88	-32.50	-151.45
BEL	51.83	20.80	50.05	105.18
BMT	40.30	116.20	30.22	-172.55
BOU	40.13	-105.23	48.05	-38.67
CLF	48.02	2.26	49.56	85.72
CMO	64.87	-147.86	65.36	-97.23
EYR	-43.42	172.35	-46.79	-106.06
HER	-34.41	19.23	-33.89	84.68
HON	21.32	-158.00	21.59	-89.70
KAK	36.23	140.18	27.46	-150.78
SJG	18.12	-66.15	27.93	6.53
VSS	-22.40	-43.65	-13.43	27.06

Source: <http://wdc.kugi.kyoto-u.ac.jp/igrf/gggm/index.html> (2010)

190 terize the global diurnal variation behavior. To identify periods of magnetic  
191 disturbance, we use the discrete wavelet transform. This technique is em-  
192 ployed to analyze the removal of disturbed days from the magnetograms, and  
193 consequently, from the reconstructed Sq signal. Also in this section, a com-  
194 bined methodology using the PCA and gapped wavelet transform is briefly  
195 described. Following, we present an identification method to distinguish the  
196 disturbed days using discrete wavelet coefficients.

198 Among the several available methods of analysis, PCA is a particularly  
199 useful tool in studying large quantities of multi-variate data. PCA is used  
200 to decompose a time-series into its orthogonal component modes, the first of  
201 which can be used to describe the dominant patterns of variance in the time  
202 series Murray (1984). The PCA is able also to reduce the original data set  
203 of two or more observed variables by identifying the significant information  
204 from the data. Principal Components (PCs) are derived as the eigenvectors of  
205 the correlation matrix between the variables. Their forms depend directly on  
206 the interrelationships existing within the data itself. The first PC is a linear  
207 combination of the original variables, which when used as a linear predictor  
208 of these variables, explains the largest fraction of the total variance. The  
209 second, third PC, etc., explain the largest parts of the remaining variance  
210 Murray (1984).

211 As explained by Yamada (2002), the interpretation of the eigenvectors  
212 and the eigenvalues can be described as follow, the eigenvectors are the nor-  
213 malized orthogonal basis in phase space, and also, the set of vectors of the  
214 new coordinate system in the space, different from the coordinate system of  
215 the original variables; the eigenvalues are the corresponding variance of the  
216 distribution of the projections in the new basis.

217 In order to isolate the global contributions of each PCs mode, we applied  
218 PCA using the wavelet correlation matrix computed by gapped wavelet trans-  
219 form. This wavelet correlation matrix was introduced in Nesme-Ribes et al.  
220 (1995). We joined the properties of the PCA, which are the compression of  
221 large databases and the simplification by the PCs modes, and properties of

222 the wavelet correlation matrix, which is the correlation at a given scale,  $a$ ,  
223 in this case, the scale corresponded to the pseudo-period of 24 hours.

#### 224 *Identification of magnetic disturbance*

225 The wavelet analysis has the following propriety: the larger amplitudes of  
226 the wavelet coefficients are associated with locally abrupt signal changes or  
227 “details” of higher frequency. In the work of Mendes et al. (2005b) and the  
228 following work of Mendes da Costa et al. (2011), a method for the detection  
229 of the transition region and the exactly location of this discontinuities due  
230 to geomagnetic storms was implemented. In these cases, the highest ampli-  
231 tudes of the wavelet coefficients indicate the singularities on the geomagnetic  
232 signal in association with the disturbed periods. On the other hand, when  
233 the magnetosphere is under quiet conditions for the geomagnetic signal, the  
234 wavelet coefficients show very small amplitudes. In this work, we applied this  
235 methodology with Daubechies orthogonal wavelet function of order 2 on the  
236 one minute time resolution with the pseudo-periods of the first three levels  
237 of 3, 6 and 12 minutes.

### 238 **5. Results and Discussion**

239 In this section, we will present the results of reconstructed baseline for the  
240 global quiet days variation using PCA technique implemented with gapped  
241 wavelet transform and wavelet correlation. Also, we will apply DWT to eval-  
242 uate the day-by-day level of geomagnetic disturbance using KAK magnetic  
243 station as reference.

244 Fig. 2 shows an example of the geomagnetic behavior presented at the  
245 June, 2007 magnetogram of Kakioka using continuous gapped wavelet trans-

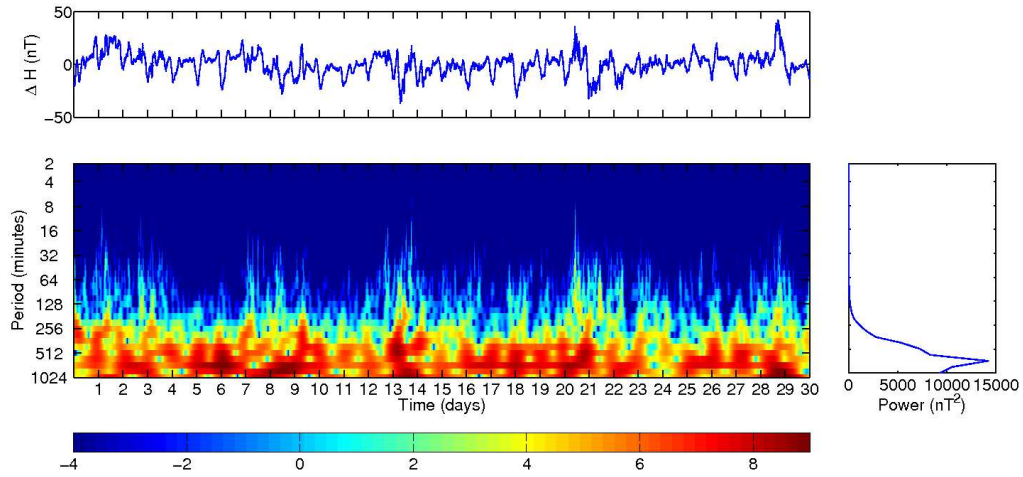


Figure 2: The GWT analysis of KAK magnetogram. At top, it shows the H-component of KAK at June, 2007 used for the wavelet analysis, at bottom left, the scalogram using Morlet wavelet, logarithmic scaled representing  $\log 2(|W(a, b)|)$ , and at bottom right, the global wavelet spectrum.

246 form (GWT). The GWT can be used in the analysis of non-stationary signal  
 247 to obtain information on the frequency or scale variations and to detect its  
 248 structures localization in time and/or in space (see Klausner et al., 2011a,  
 249 for more details). It is possible to analyze a signal in a time-scale plane,  
 250 called so the wavelet scalogram. In analogy with the Fourier analysis, the  
 251 square modulus of the wavelet coefficient,  $|W(a, b)|^2$ , is used to provide the  
 252 energy distribution in the time-scale plane. In the GWT analysis, we can also  
 253 explore the central frequencies of the time series through the global wavelet  
 254 spectrum which is the variance average at each scale over the whole time  
 255 series, to compare the spectral power at different scales. This figure shows  
 256 the H-component (top), the wavelet square modulus (bottom left) and the  
 257 global wavelet spectrum (total energy in each scale – bottom right). In the

258 scalogram, areas of stronger wavelet power are shown in dark red on a plot  
259 of time (horizontally) and time scale (vertically). The areas of low wavelet  
260 power are shown in dark blue.

261 In Fig. 2, it is possible to notice peaks of wavelet power on the scalogram  
262 at the time scale corresponding to 8 to 16 minutes of period. This periods are  
263 associated to PC5 pulsations during disturbed periods. Also, it is possible  
264 to notice a maximum of wavelet power at the time scale corresponding to  
265 harmonic periods of the 24 hours such as 6, 8, 12 hours. Those periods are  
266 related to the diurnal variations.

267 The GWT technique is able to analyze all the informations present on the  
268 magnetograms. It is an auxiliary tool to localize on time/space the PC1–PC5  
269 pulsations (Saito, 1969). However, the scalogram provides a very redundancy  
270 information which difficult the analysis of each decoupling phenomenon. For  
271 that reason, we preferred to use DWT to evaluate the day-by-day level of  
272 geomagnetic disturbance.

273 Fig. 3 is composed of two graphs, the first one presents the reconstructed  
274 line of the Sq variation where the first 10 geomagnetically quietest days of  
275 each month are highlighted in blue and the 5 most disturbed days in red  
276 and the second one presents the discrete wavelet analysis of the geomagnetic  
277 horizontal component obtained at Kakioka station, Japan.

278 Using our criteria of removing disturbed days, we consider as gaps of 3rd,  
279 14th, 21th and 29th day. In our case, the gapped wavelet technique is very  
280 helpful because it reduces two effects: the presence of gaps and the boundary  
281 effects due to the finite length of the data, for more details see Klausner et al.  
282 (2011a).

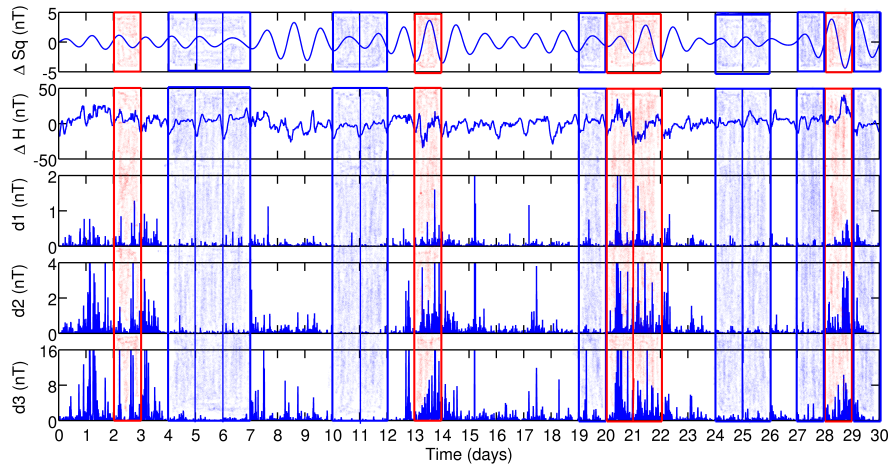


Figure 3: The amplitude variation of the reconstructed Sq signal with the highlighted 10 geomagnetically quietest days (blue) and 5 most disturbed days (red), the H-component average variation for KAK obtained at June, 2007 and the square root wavelet coefficients amplitudes  $d1$ ,  $d2$  and  $d3$  with the pseudo-periods of 3, 6 and 12 minutes.

283 The first graph shows the amplitude range between  $-5$  and  $5$  nT and  
 284 presents a complex pattern. It is possible to notice that the larger amplitudes  
 285 of the reconstructed Sq signal correspond to the periods between the days  
 286  $8-10$ ,  $13-15$ ,  $21-23$  and  $29-30$ . These periods correspond to the disturbed  
 287 days.

288 Table 5 shows these 10 quietest days and 5 most disturbed days of each  
 289 month set by the *GeoForschungsZentrum (GFZ) Potsdam* through the anal-  
 290 ysis of the Kp index that are highlighted on the second graph. The year  
 291 of 2007 is a representative year of minimum solar activity and it is used in  
 292 this analysis due to have less disturbed periods (see our considerations in  
 293 Section 3). By analyzing these highlighted days, we expect to find out if  
 294 there is a correlation between the days classified as quiet days and a small



295 Sq amplitude variation.

Table 2: The first 10 geomagnetically quietest days and first 5 most disturbed days set by the *GeoForschungsZentrum (GFZ) Potsdam*

Month/year	10 quietest days										5 most disturbed days				
	q1	q2	q3	q4	q5	q6	q7	q8	q9	q10	d1	d2	d3	d4	d5
Mar	20	21	3	19	9	29	22	18	31	4	13	24	6	7	14
Jun	5	12	6	7	11	26	25	20	30	28	14	21	22	3	29
Sep	13	9	10	11	12	16	17	19	26	15	29	2	28	23	27
Dec	3	8	4	25	7	26	2	29	15	6	18	17	11	20	21

SOURCE: <http://wdc.kugi.kyoto-u.ac.jp/qddays/index.html>.

296 The second graph shows the discrete wavelet analysis applied to geo-  
 297 magnetic minutely signal from KAK using Daubechies orthogonal wavelet  
 298 family 2. From top to bottom in this graph, the H-component of the geo-  
 299 omagnetic field and the first three levels of the square wavelet coefficients  
 300 denoted by d1, d2 and d3. This analysis uses the methodology developed  
 301 by Mendes et al. (2005b), and posteriorly applied by Mendes da Costa et al.  
 302 (2011) and Klausner et al. (2011b).

303 In order to facilitate the evaluation of the quiet periods obtained by the  
 304 discrete wavelet analysis applied to geomagnetic signal from KAK, we also  
 305 developed a methodology (effectiveness wavelet coefficients (EWC)) to in-  
 306 terpret the results shown in Fig. 4. The EWC corresponds to the weighted  
 307 geometric mean of the square wavelet coefficients per hour. It is accom-  
 308 plished by weighting the square wavelet coefficients means in each level of  
 309 decomposition as following

$$EWC = \frac{4 \sum_{i=1}^N d1 + 2 \sum_{i=1}^N d2 + \sum_{i=1}^N d3}{7}, \quad (3)$$

310 where  $N$  is equal to 60 because our time series has one minute resolution.

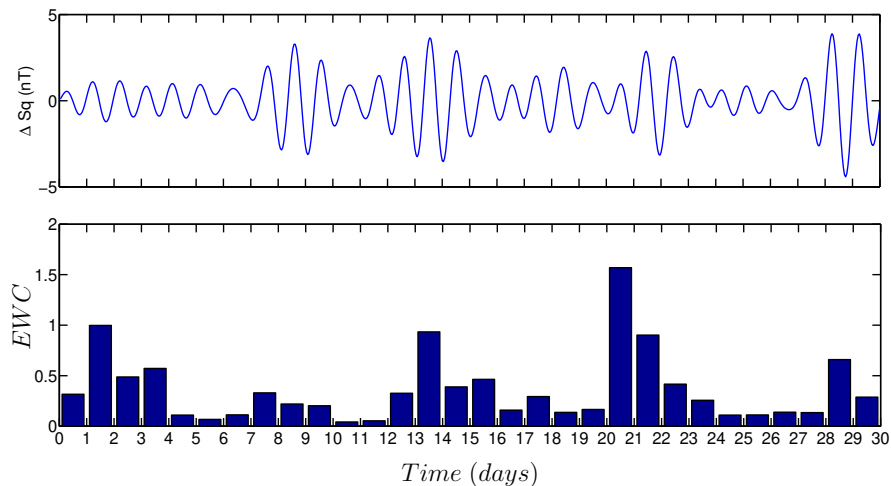


Figure 4: The comparative of the global Sq behavior and the effectiveness wavelet coefficients for the month of June, 2007.

311 Through Fig. 4, it is possible to compare the global Sq behavior (top  
 312 graph) with the analysis of quiet and disturbed days obtained by one repre-  
 313 sentative magnetic station of medium/low latitudes (KAK – bottom graph)  
 314 in order to verify situations in which the global Sq behavior presents less  
 315 or more variability. This analysis allows us to validate the quietest days,  
 316 and evaluate the most disturbed days in order to establish a reliable method  
 317 of global Sq analysis obtained from medium/low latitude magnetic stations  
 318 influenced only by the ionosphere.

319 In Fig. 4, the global Sq behavior (top graph) shows larger amplitudes  
 320 during the periods between the days 8–10, 12–16, 22–23 and 29–30. Most  
 321 of these periods correspond to the days where the EWCs have an increase  
 322 of their values as shown KAK analysis (bottom graph). The increase of the  
 323 EWCs values occurs during the periods between the days 1–4, 8–10, 13–18,

324 21–24 and 29–30. The EWCs can help us also to interpret the results obtained  
 325 in each day, and can help us to evaluate the quietest and most disturbed days  
 326 measure by the selected magnetic station of medium/low latitudes, KAK, as  
 327 shown in Table 5.

Table 3: The 10 geomagnetically quietest days and 5 most disturbed days obtained by the discrete wavelet analysis

Month/year	10 quietest days										5 most disturbed days				
	q1	q2	q3	q4	q5	q6	q7	q8	q9	q10	d1	d2	d3	d4	d5
Mar	3	10	20	9	21	8	2	19	22	4	13	25	12	15	24
Jun	11	12	6	25	5	26	7	28	19	27	21	2	14	22	29
Sep	12	11	10	9	17	18	16	13	26	19	27	22	29	2	20
Dec	25	7	3	8	1	24	4	6	16	28	17	18	11	20	10

328 The same methodology and analysis comparing the global Sq behavior  
 329 and the EWCs from KAK is done for the month of March, September and  
 330 December,2007.

331 Fig. 5 shows the comparative of the global Sq behavior and the EWCs  
 332 from KAK for the month of March, 2007. The amplitude range of global  
 333 Sq signal is between  $-15$  and  $15$  nT, and, it also shows a complex pattern.  
 334 It is possible to notice that the larger amplitudes of the reconstructed Sq  
 335 signal correspond to the periods between the days 6–7, 11–17 and 23–28.  
 336 Once more, these periods correspond to the disturbed days. The increase of  
 337 the EWCs values occurs during the periods between the days 1, 6–7, 11–17,  
 338 23–28 and 30–31. We can notice that the increase of the amplitude of the  
 339 reconstructed Sq signal correspond to the increase of the EWCs magnitude.

340 The amplitude range for September, 2007, is between  $-15$  and  $15$  nT  
 341 and the larger amplitudes of the reconstructed Sq signal correspond to the  
 342 periods between the days 1–7, 19–23 and 26–30, see Fig. 6. The increase of

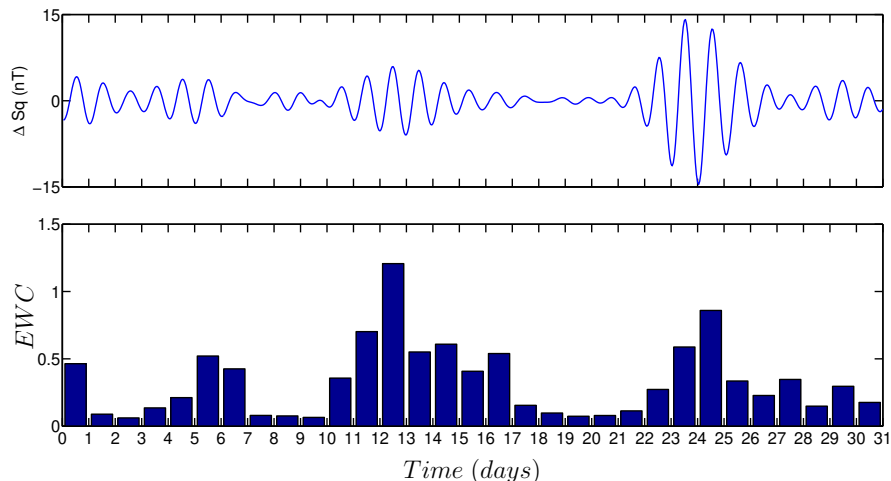


Figure 5: The comparative of the global Sq behavior and the effectiveness wavelet coefficients for the month of March, 2007

343 the EWCs values occurs during the periods between the days 1–3, 20–24 and  
 344 27–30. Comparing these two analysis, the global and the EWCs, we verify  
 345 that the KAK magnetic behavior represents well the increase of global Sq  
 346 oscillations.

347 In Fig. 7, the amplitude range is between  $-10$  and  $10$  nT and the larger  
 348 amplitudes correspond to the periods between the days 15–23. Also, the  
 349 increase of the EWCs values occur during the periods between the days 10–  
 350 11 and 17–21. Once more, when we compare these two analysis, the global  
 351 and the EWCs, we verify that the KAK magnetic behavior represents well  
 352 the increase of global Sq oscillations.

353 We observe in Figs. 4, 5, 6 and 7, in most of the cases, the major am-  
 354 plitude fluctuations of the reconstructed Sq signal correspond to the most  
 355 disturbed days and minor fluctuations, to the quietest days. However, the

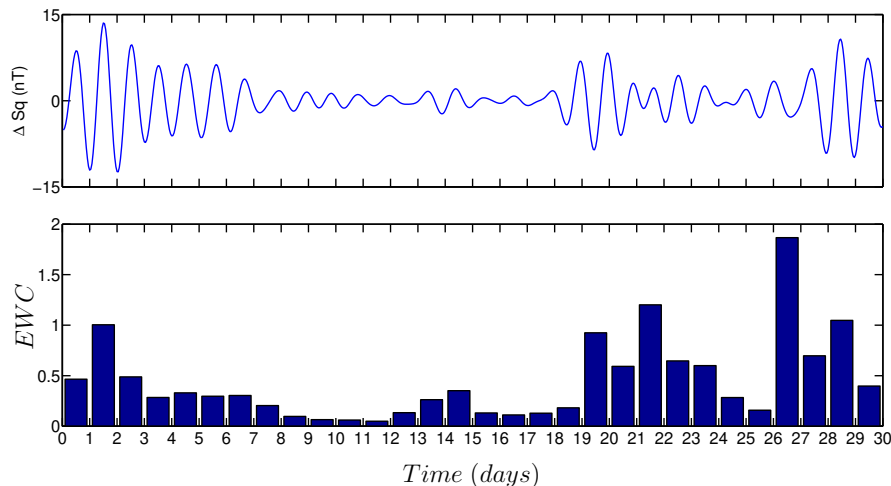


Figure 6: The comparative of the global Sq behavior and the effectiveness wavelet coefficients for the month of September, 2007

356 diurnal global variability shows a complexity on the amplitude variation pat-  
 357 tern even during geomagnetically quiet periods. Through this study we com-  
 358 pare the amplitude variation of the reconstructed Sq signal to effectiveness  
 359 wavelet coefficients obtained at KAK with the purpose of understanding the  
 360 complexity of the diurnal global variability.

## 361 6. Conclusions

362 In this work, we suggest an alternative approach for the calculation of the  
 363 Sq baseline using wavelet and PCA techniques. This new approach address  
 364 some issues, such as, the availability and the quality of data, abrupt changes  
 365 in the level of the H-component, erroneous points in the database and the  
 366 presence of gaps in almost all the magnetic observatories. To fulfill this  
 367 purpose, we reconstruct the Sq baseline using the wavelet correlation matrix

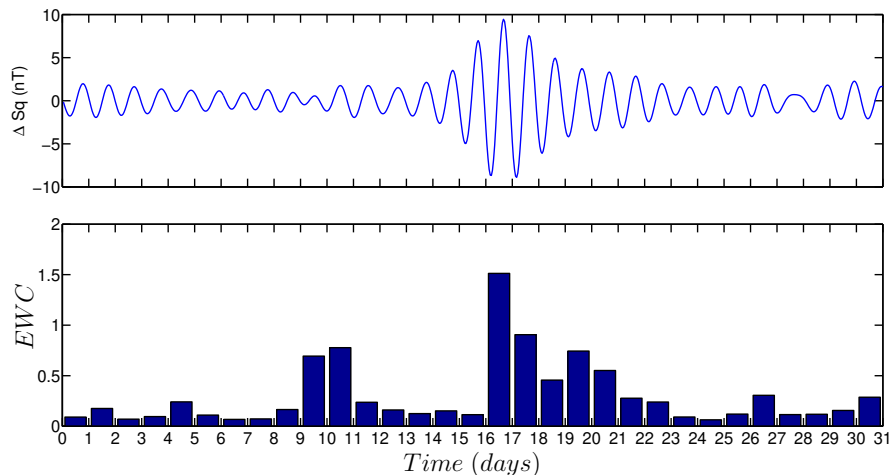


Figure 7: The comparative of the global Sq behavior and the effectiveness wavelet coefficients for the month of December, 2007

368 with scale of 24 hours (pseudo-period). The PCA/wavelet method uses the  
 369 global variation of first PCA mode that also corresponds to phenomena with  
 370 periods of 24 hours. This study shows that the largest amplitude oscillation  
 371 of the reconstructed signal (Sq baseline) corresponded to the most disturbed  
 372 days and the smaller oscillations to the quietest days. This result is consistent  
 373 with the expected Sq variations.

## 374 7. Acknowledgments

375 V. Klausner wishes to thanks CAPES for the financial support of her  
 376 PhD (CAPES – grants 465/2008) and her Postdoctoral research (FAPESP –  
 377 2011/20588-7). This work was supported by CNPq (grants 309017/2007-6,  
 378 486165/2006-0, 308680/2007-3, 478707/2003, 477819/2003-6, 382465/01-6),  
 379 FAPESP (grants 2007/07723-7) and CAPES (grants 86/2010-29, 0880/08-6,

380 86/2010-29, 551006/2011-0, 17002/2012-8). Also, the authors would like to  
381 thank the INTERMAGNET programme for the datasets used in this work.

## 382 **References**

383 Bartels, J., 1957. The technique of scaling indices  $k$  and  $q$  of geomagnetic  
384 activity. *Annals of the International Geophysical Year* (4), 215–226.

385 Burton, R. K., McPherron, R. L., Russell, C. T., 1975. An empirical relation-  
386 ship between interplanetary conditions and Dst. *Journal of Geophysical*  
387 *Research*, 80 (1), pp. 4204–4214.

388 Campbell, W. H., 1997. *Introduction to Geomagnetic Fields*. Cambridge Uni-  
389 versity Press, New York.

390 Domingues, M. O., Mendes, O. J., Mendes da Costa, A., 2005. Wavelet  
391 techniques in atmospheric sciences. *Advances in Space Research* 35 (5),  
392 831–842.

393 Gonzalez, W. D., Joselyn, J. A., Kamide, Y., Kroehl, H. W., Rostoker, G.,  
394 Tsurutani, B. T., Vasyliunas, V. M., 1994. What is a geomagnetic storm?  
395 *Journal of Geophysical Research*, 99 (A4), pp. 5771–5792.

396 Kamide, Y., Baumjohann, W., Daglis, I. A., Gonzalez, W. D., Grande, M.,  
397 Joselyn, J. A., McPherron, R. L., Phillips, J. L., Reeves, E. G. D., Ros-  
398 toker, G., Sharma, A. S., Singer, H. J., Tsurutani, B. T., and Vasyliunas,  
399 V. M., 1998. Current understanding of magnetic storms: Storm-substorm  
400 relationships. *Journal of Geophysical Research*, 103 (A8), pp. 17705–17713.

- 401 Karinen, A., Mursula, K., 2005. A new reconstruction of the Dst index for  
402 1932-2002. *Annales Geophysicae*, 23, pp 475–485.
- 403 Karinen, A., Mursula, K., 2006. Correcting the Dst index: Consequences  
404 for absolute level and correlations. *Journal of Geophysical Research*,  
405 111 (A08207).
- 406 Klausner, V., Papa, A. R. R., Mendes, O., Domingues, M. O., Frick, P.,  
407 2011a. Characteristics of solar diurnal variations: a case study based  
408 on records from the ground magnetic observatory at Vassouras, Brazil.  
409 arXiv:1108.4594 [physics.space-ph].
- 410 Klausner, V., Domingues, M. O., Mendes, O., Papa, A. R. R.,  
411 2011b. Tsunami effects on the Z component of the geomagnetic field.  
412 arXiv:1108.4893v1 [physics.space-ph]
- 413 Love, J. J., Gannon, J. L., 2009. Revised Dst and the epicycles of magnetic  
414 disturbance: 19582007. *Annales Geophysicae* 27, pp. 3101–3131.
- 415 Mendes, O. J., Domingues, M. O., Mendes da Costa, A., Clúa de Gonza-  
416 lez, A. L., 2005a. Wavelet analysis applied to magnetograms: Singular-  
417 ity detections related to geomagnetic storms. *Journal of Atmospheric and*  
418 *Solar-Terrestrial Physics*, 67, pp. 1827–1836.
- 419 Mendes, O. J., Mendes da Costa, A., Domingues, M. O., 2005b. Introduction  
420 to planetary electrodynamics: a view of electric fields, currents and related  
421 magnetic fields. *Advances in Space Research*, 35 (5), pp. 812-818.
- 422 Mendes da Costa, A., Domingues, M. O., Mendes, O., Brum, C. G. M.,



423 2011. Interplanetary medium condition effects in the south atlantic mag-  
424 netic anomaly: A case study. *Journal of Atmospheric and Solar-Terrestrial*  
425 *Physics*, 73 (11–12), pp. 1478–1491.

426 Murray, G. W.; Mueller, J. C.; Zwally, H. J., 1984 Matrix partitioning and  
427 EOF/Principal Components Analysis of Antarctic Sea Ice Brightness Tem-  
428 peratures. Greenbelt, Md. : National Aeronautics and Space Administra-  
429 tion, Goddard Space Flight Center, 1 v., NASA technical memorandum,  
430 83916.

431 Mursula, K., Holappa, L., Karinen, A., 2008. Correct normalization of the  
432 Dst index. *Astrophysics and Space Sciences Transactions*, 4 (2), pp.41–45.

433 Mursula, K., Holappa, L., Karinen, A., 2010. Uneven weighting of stations  
434 in the Dst index. *Journal of Atmospheric and Solar-Terrestrial Physics*,  
435 73 (2-3), pp. 316–322.

436 Nesme-Ribes, E., Frick, P., Sokoloff, D., Zakharov, V., Ribes, J. C.,  
437 Vigouroux, A., Laclare, F., 1995. Wavelet analysis of the maunder mini-  
438 mum as recorded in solar diameter data. *Comptes rendus de l’Académie*  
439 *des sciences. Série II, Mécanique, physique, chimie, astronomie* 321 (12),  
440 525–532.

441 Saito, T., 1969. Geomagnetic pulsations. *Space Science Reviews*, 10 (3), pp.  
442 319–412.

443 Yamada, K., 2002. 2-day, 3-day, and 5-6-day oscillations of the geomagnetic  
444 field detected by principal component analysis. *Earth Planets Space* 54  
445 (4), 379–392.